

Relative Contagiousness of Emerging Virus Variants: An Analysis of the Alpha, Delta, and Omicron SARS-CoV-2 Variants *

Peter Reinhard Hansen^{a,b}

^a*University of North Carolina*[†]

^b*Copenhagen Business School*

January 21, 2022

Abstract

We propose a simple dynamic model for estimating the relative contagiousness of two virus variants. Maximum likelihood estimation and inference is conveniently invariant to variation in the total number of cases over the sample period and can be expressed as a logistic regression. We apply the model to Danish SARS-CoV-2 variant data. We estimate the reproduction numbers of Alpha and Delta to be larger than that of the ancestral variant by a factor of 1.51 [CI 95%: 1.50, 1.53] and 3.28 [CI 95%: 3.01, 3.58], respectively. In a predominately vaccinated population, we estimate Omicron to be 3.15 [CI 95%: 2.83, 3.50] times more infectious than Delta.

Forecasting the proportion of an emerging virus variant is straight forward and we proceed to show how the effective reproduction number for a new variant can be estimated without contemporary sequencing results. This is useful for assessing the state of the pandemic in real time as we illustrate empirically with the inferred effective reproduction number for the Alpha variant.

Keywords: COVID-19, SARS-CoV-2, Reproduction number, Alpha variant, Delta variant, Omicron variant, B.1.1.7, B.1.617.2, B.1.1.529, Maximum Likelihood, Logistic Regression.

*Thanks to Torben Andersen, Victor Chernozhukov, Peter Dalggaard, Emily Dyckman, Claus Ekstrøm, Mogens Fosgerau, Ulrik Gerdes, Martin Vinæs Larsen, Serena Ng, Uffe Poulsen, Morten Rasmussen, and Tom Wenseleers for valuable comments and suggestions. I also thank anonymous reviewers for valuable comments and suggestions and David Sanders and Michael Krabbe Borregaard for making tutorials and information about the Julia language available and the Danish Patient Safety Authority for sharing data on COVID-19 cases in relation to Euro 2020 games.

[†]Address: University of North Carolina, Department of Economics, 107 Gardner Hall Chapel Hill, NC 27599-3305

1 Introduction

During the fall of 2020, confirmed cases of COVID-19 grew rapidly in the UK with the emergence of the Alpha variant of SARS-CoV-2 (B.1.1.7) formerly known as the British variant, see Rambaut et al. (2020). The Alpha variant was shown to be more contagious than earlier lineages, see Volz et al. (2021) and Washington et al. (2021). Moreover, infection with the Alpha variant was found to increase the risk of hospitalization by about 42%, see Bager et al. (2021). India experienced a similar explosive growth in COVID-19 cases in April 2021 following the emergence of the Delta variant (B.1.617.2), formerly known as the Indian variant. The Omicron variant (B.1.1.529) was first detected on November 22, 2021 in southern Africa, see Viana et al. (2022), and has led to rapid increases in COVID-19 case numbers in many parts of the world.

In this paper, we formulate a simple model for two virus variants of an infectious disease, where the object of interest is the relative contagiousness, denoted by γ , which we will also refer to as the competitive advantage. The time series of new-variant cases to total cases can be modeled as binomially distributed variables with a time-varying parameter, λ_t . The dynamic properties of λ_t are given by the relative contagiousness that can be estimated solely from changes in the relative proportion of the two variants. The analysis is therefore invariant to the reproduction number for the existing lineage and time variation therein. This is convenient because the reproduction number varies substantially over time due to changes in behavior and preventive measures along with other factors. The analysis is also invariant to testing intensity and time variation therein, so long as the variation in sampling does not “favor” one variant over another. Our starting point is maximum likelihood analysis of the sequenced tests, which leads to a simple logistic regression after some straight forward algebra. This greatly simplifies the estimation, inference, and prediction.¹

The *basic reproduction number*, R_0 , is an important characteristic of an infectious disease and during a pandemic the *effective reproduction number*, R_t , provides a measure of the direction for case numbers during the pandemic. The time it takes to determine the genome in positive cases present an obstacle for assessing the reproduction number for a new virus variant. Such data are typically only available with some delay. We show that the highly predictable nature of the proportion of a new variant can be used to infer its reproduction number from the aggregate reproduction number and the most recently available estimate of the proportion, λ . The effective reproduction number for all cases is simpler to compute and the proportion of a new variant can be projected forward, typically with high accuracy.

¹A early draft with these results were first shared on January 26, 2021, <https://twitter.com/ProfPHansen/status/1353808634652708864> and a YouTube presentation of these results and an analysis of the Alpha variant (B.1.1.7) was shared on February 14, 2021. <https://www.youtube.com/watch?v=u5kkwe3aXLM>

This makes it possible to compute the effective reproduction number of a new variant with a simple formula before contemporaneous sequencing results are available.

We apply the methodology to Danish data and study the Alpha and Delta variants using weekly data, whereas daily data are used to study the swiftly progressing Omicron variant. The Danish data are excellent for studying the progression of a new variant of SARS-COV-2 because the vast majority of confirmed COVID-19 cases were sequenced during the periods where each of the three variants emerged. Moreover, testing is extensive in Denmark. During the three sample periods, the number of weekly PCR tests varied between nearly 500 thousands and over 1.5 million tests per week for a population of about 5.8 million individuals. The proportion of the new-variant cases increased from $<0.5\%$ to over 90% during the sample periods for the Alpha and Delta variants, see Figure 1, and from $<2\%$ to over 90% during the sample period for the Omicron variant. The progression of the Alpha variant is shown in the left panel Figure 1 and the progression of the Delta variant in the right panel, along with 95% confidence intervals for each week. It can be seen that the Delta variant progressed substantially faster than the Alpha variant. For instance, it took the Alpha variant about eight weeks to increase from $<10\%$ to $>90\%$, while this same growth was achieved by the Delta variant in just 4 weeks. The Omicron variant progressed even faster as we show below. On December 8th, 2021, just 16 days after Omicron was first detected in southern Africa, the Omicron variant accounted for over 10% of COVID-19 cases in Denmark and 19 days later, on December 28, 2021, the new variant accounted for 90% of all COVID19 cases, see Table 3.

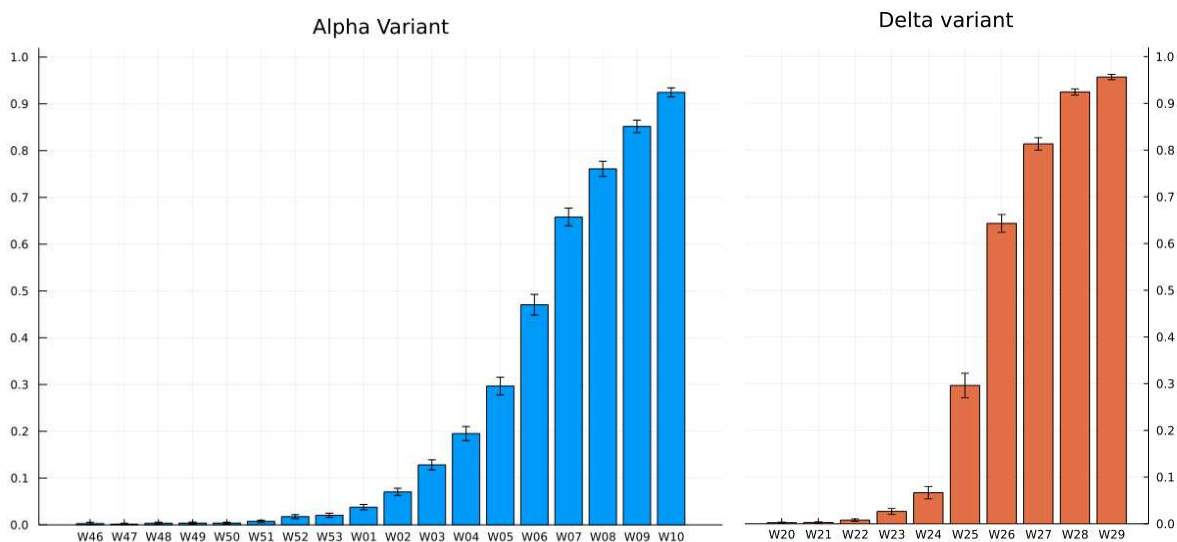


Figure 1: Weekly proportions of Alpha and Delta variants relative to all cases.

The paper is organized as follows: We present the statistical model in Section 2, where the time

series of binomially distributed variables is expressed as a logistic regression. We present the data and the empirical results on relative contagiousness in Section 3. Section 4 presents the two auxiliary results on prediction and inferring the latent reproduction number for a new emerging variant. We illustrate how the proportion of new-variant cases can be predicted and derive the associated confidence bands. We apply this to the Alpha variant data and review how accurate the estimated model was at predicting the realized proportion of the Alpha variant out-of-sample. Then we derive the method for estimating the latent reproduction number for a new emerging variant and apply the method to the Alpha variant data. Section 5 has some concluding remarks, and we present extensions and some details about the maximum likelihood estimation and robust standard errors in the Appendix B.

2 The Statistical Model

In this section we present the simple dynamic structure for the case numbers of two competing virus variants. The structure is not specific to competing virus variants, but could be used to analyze other competing objects. The extension to the situation with more than two competing variants is derived in Appendix A.

2.1 Two Competing Virus Variants

Consider a virus with two variants, A and B , and let R_0^A and R_0^B denote their basic reproduction numbers. We use B to represent a new, emerging variant whereas A represents the older variant. The parameter of interest is the relative contagiousness, defined by $\gamma = R_0^B/R_0^A$.

Suppose that the number of new cases in period t are denoted A_t and B_t , respectively. The rate of growth in case numbers for the old variant is denoted, $a_t = A_t/A_{t-1}$, which depends on its contagiousness and the number of “opportunities” the virus has to jump from an infected individual to another person. The latter is heavily influenced by preventive measures and restrictions imposed by health authorities, seasonality, percentage of susceptible people in the population, individual behavior, along with many other things. The new virus variant is subject to the same level of “opportunities”, and only differs in terms of its contagiousness, such that the ratio of effective reproduction numbers is constant and equal to, $\gamma = R_t^B/R_t^A$. It follows that variant B ’s rate of growth is proportional to a_t , and given by

$$b_t = B_t/B_{t-1} = \gamma a_t.$$

The observed data are the detected cases for which the genome is determined. In period t , the

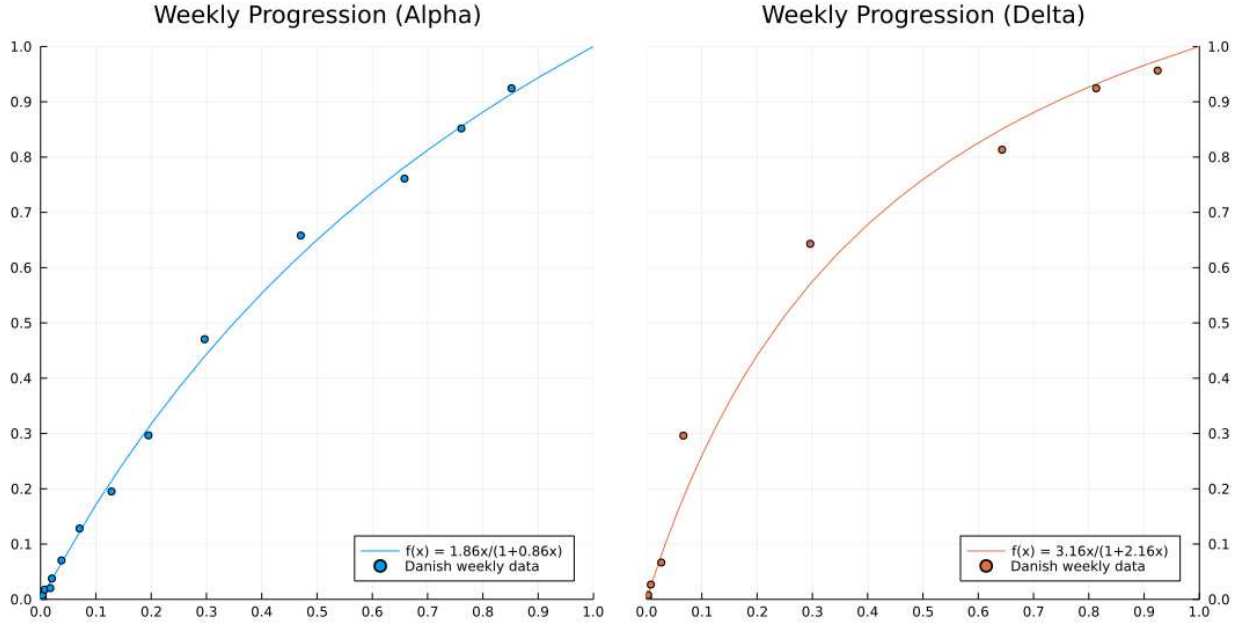


Figure 2: Proportion of the new variant against that of the previous week.

genome is determined in N_t of the new cases, where X_t are variant B and $N_t - X_t$ are variant A . We assume N_t is a representative random sample from the population of new cases such that $X_t \sim \text{Bin}(N_t, \lambda_t)$, with $\lambda_t = \frac{B_t}{A_t+B_t}$. It follows that

$$\begin{aligned} \lambda_{t+1} &= \frac{B_{t+1}}{A_{t+1} + B_{t+1}} = \frac{\gamma a_{t+1} B_t}{a_{t+1} A_t + \gamma a_{t+1} B_t} \\ &= \frac{\gamma B_t / (A_t + B_t)}{A_t / (A_t + B_t) + \gamma B_t / (A_t + B_t)} = \frac{\gamma \lambda_t}{(1 - \lambda_t) + \gamma \lambda_t}. \end{aligned} \quad (1)$$

Note that the dynamic equation for λ_t depends on the ratio $\gamma = b_t/a_t$ but not the actual values of a_t and b_t . This greatly simplifies the analysis and estimation and inference about γ becomes invariant to a range of changes during the sample period that influence the rate of change in case numbers. Equation (1) defines the function $f(x) = \gamma x/[1 + (\gamma - 1)x]$ that characterizes the expected progression of a new variant. Figure 2 presents two examples of $f(x)$, which is strictly increasing for $\gamma > 1$. The case $\gamma = 1.86$ is shown in the left panel and $\gamma = 3.16$ in the right panel along with the progression of the weekly observed progression of the Alpha (left) and Delta (right) variants, where the proportion of the new variant this week (y-axis) is plotted against its proportion in the previous week (x-axis).

The progression of a very contagious variant can seem deceptively slow in the early phase. If we take the case $\gamma = 1.86$, which is our estimate for the Alpha variant, then it takes four weeks for the new variant to increase from 1 in 1,000 cases to 1 in a 100 cases. Then another four weeks to increase to 1 in 10 cases. After that, it picks up the pace and the new variant becomes the dominant variant

($\lambda_t > 50\%$) four weeks later and reaches +90% of all cases after another four weeks. So, it can take months from the moment the first case of a new and more contagious variant is observed to the time when the new variant begins to have a noticeable impact on the total number of cases. After the new variant becomes dominant it can radically change the momentum of the pandemic. A relatively stable period can suddenly become one where cases grow exponentially, because the new dominant variant has a larger reproduction number. This scenario played out for both the Alpha, Delta, and Omicron variants in many places, such as the August 2021 large surge in Delta cases in Florida, Texas, along with other states in the US.

2.2 The Likelihood Analysis and Logistic Regression

Let N_t denote the total number of new cases in period t for which the genome is identified, and let X_t be the number of cases that are identified as the new emerging variant. We assume that X_t is binomially distributed, $\text{Bin}(N_t, \lambda_t)$, where λ_t evolves according to (1). This requires that the variant is identified in a representative sample of positive cases for all t . In the absence of serial dependence, the log-likelihood function for the sample (N_t, X_t) , $t = 1, \dots, T$, is proportional to

$$\ell(\gamma, \lambda_0) \propto \sum_{t=1}^T X_t \log \lambda_t + (N_t - X_t) \log(1 - \lambda_t).$$

The two unknown parameters, the initial value $\lambda_0 \equiv \lambda$ and γ , can be estimated by maximum likelihood, $(\hat{\lambda}, \hat{\gamma}) = \arg \max_{\gamma, \lambda} \ell(\lambda, \gamma)$, and confidence intervals for λ and γ can be obtained with conventional methods. The likelihood can conveniently be expressed as a logistic regression model. For this purpose, we introduce the odds ratio, $\rho_t = \lambda_t / (1 - \lambda_t)$, and it is simple to show that (1) is equivalent to the simple dynamic equation, $\rho_t = \gamma \rho_{t-1}$. This implies that

$$\rho_t = \gamma^t \rho_0 = \exp(\log \rho_0 + \log \gamma \times t) = \exp(\alpha + \beta t),$$

where $\alpha = \log \rho_0$ and $\beta = \log \gamma$. Since $\lambda_t = \rho_t / (1 + \rho_t)$, the structure of the logistic regression model emerges such that

$$\lambda_t = \frac{\exp(\alpha + \beta t)}{1 + \exp(\alpha + \beta t)} = \frac{1}{1 + e^{-\alpha - \beta t}}. \quad (2)$$

This model is straight forward to estimate and analyze using standard software implementations, including the generalized linear model package, `glm`, that is implemented in R and Julia. In the empirical analysis we estimate the model by maximum likelihood and compute robust standard errors from

the score and hessian of the log-likelihood function, see White (1994). While heteroskedasticity is a natural feature of binomially distributed random variables with a time-varying probability, λ_t , distributional misspecification can invalidate the non-robust standard errors. Dynamic misspecification where $\lambda_t = (1 + e^{-\alpha - \beta t})^{-1}$ does not hold for all t can result in inconsistent estimates. The details are presented in Appendix B.²

3 Empirical Analyses of the Alpha, Delta, and Omicron Variants

Data for the sequenced COVID-19 tests were obtained from the Statens Serum Institut (SSI), Denmark. We use the weekly data to analyze the Alpha and Delta variants and daily data to analyze the Omicron variant.³

The majority of positive COVID-19 tests had their genome identified in Denmark during the three sample periods, with the exception of the last third of the daily Omicron data, where SSI determined the variant in a representative sample of positive PCR tests.

3.1 Alpha and Delta Variants

Table 1 presents the the weekly numbers of PCR COVID-19 tests, the number of positive tests, C_t , the number of tests with the genome identified, N_t , and the number of tests for which the new emerging variant was found, X_t , along with the percentages of positive tests for which the genome was determined and the percentage of these tests that were the new variant.

The first sample period, November 9, 2020 to March 14, 2021 (18 weeks), is the period where the Alpha variant made its inroad in Denmark, the second sample period, May 17 to July 25, 2021 (10 weeks), is the period where the Delta variant grew to dominance in Denmark.

A preliminary probing of the data can be done by considering the empirical odds ratios of new-variant cases to old-variant cases. This ratio should be approximately proportional to B_t/A_t , such that the ratio of consecutive odds ratios,

$$\frac{X_t}{N_t - X_t} \bigg/ \frac{X_{t-1}}{N_{t-1} - X_{t-1}} = \frac{X_t/X_{t-1}}{(N_t - X_t)/(N_{t-1} - X_{t-1})} \approx b_t/a_t = \gamma.$$

²Identical estimates were obtained with the `glm` packaged in Julia, see Besançon et al. (2019) and Lin et al. (2021). The proper command for the `glm` package in Julia is: `glm(@formula(x / n ~ time_trend), [data], wts = n, Binomial())` and in R it is: `glm(x/n ~ tt, weights=n, [data], family = binomial)`, see R Core Team (2018) for details. The latter was kindly provided by Peter Dalggaard. The `glm` package computes the non-robust standard errors based on the Fisher information. These were smaller than the robust standard errors, in particular in our analysis of the Delta variant. Robust and non-robust confidence intervals are reported in Appendix B.

³Replication files (Jupyter notebooks with data and Julia code) are available at github.com/reinhardhansen/VirusVariantsReplicationFiles, see Hansen (2022).

Table 1: COVID-19 PCR tests and outcomes by week

Week	Tested (PCR)	Cases C_t	Sequenced N_t (N_t/C_t)	Alpha cases X_t	Alpha proportion X_t/N_t
46	490,543	7,533	1,486 (19.7%)	4	0.27%
47	502,852	8,456	1,941 (23.0%)	3	0.15%
48	502,851	8,774	2,127 (24.2%)	7	0.33%
49	544,578	12,816	2,868 (22.4%)	11	0.38%
50	694,989	21,925	4,226 (19.3%)	16	0.38%
51	883,253	24,579	4,943 (20.1%)	37	0.75%
52	650,374	17,043	3,633 (21.3%)	64	1.76%
53	536,958	14,560	3,916 (26.9%)	80	2.04%
1	563,348	11,311	4,161 (36.8%)	157	3.77%
2	596,048	7,008	4,230 (60.4%)	298	7.04%
3	739,922	5,321	3,688 (69.3%)	473	12.83%
4	768,925	3,616	2,660 (73.6%)	519	19.51%
5	794,917	3,096	2,235 (72.2%)	663	29.66%
6	809,028	2,716	1,974 (72.7%)	929	47.06%
7	833,795	3,335	2,416 (72.4%)	1,590	65.81%
8	956,070	3,688	2,683 (72.7%)	2,042	76.11%
9	1,033,111	3,616	2,699 (74.6%)	2,299	85.18%
10	1,056,404	3,809	2,874 (75.5%)	2,657	92.45%

Week	Tested (PCR)	Cases C_t	Sequenced N_t (N_t/C_t)	Delta cases X_t	Delta proportion X_t/N_t
20	1,167,981	6,867	5,366 (78.1%)	13	0.24%
21	1,013,403	6,698	5,213 (77.8%)	15	0.29%
22	911,764	5,662	4,565 (80.6%)	36	0.79%
23	720,274	2,811	2,467 (87.8%)	66	2.68%
24	575,207	1,649	1,364 (82.7%)	91	6.67%
25	524,837	1,315	1,165 (88.6%)	345	29.61%
26	608,540	2,674	2,418 (90.4%)	1,555	64.31%
27	624,414	4,614	3,322 (72.0%)	2,702	81.34%
28	583,932	6,818	6,253 (91.7%)	5,781	92.45%
29	473,843	5,289	4,800 (90.8%)	4,591	95.65%

Note: Source is *Status for udvikling af B.1.1.7 og andre mere smitsomme varianter i Danmark*, SSI, April 7, 2021 and *Status for udvikling af SARS-CoV-2 Varianter der overvåges i Danmark* SSI, August 27, 2021. Data available at: <https://files.ssi.dk/covid19/virusvarianter/status/status-virusvarianter-07042021-dg45> and <https://files.ssi.dk/covid19/virusvarianter/status/virusvarianter-covid-19-280721-gd14>

Thus we can use the ratio of consecutive odds ratios as a measurements of γ in week t . These empirical ratios and the corresponding confidence intervals are shown in Figure 3.⁴ The horizontal dashed lines in Figure 3 represent the average value of the crude measures, which is 1.73 in for Alpha and 3.19 for Delta. The crude measures tend to have large confidence intervals early in the sample because the

⁴Weekly crude measures for NHS England STP areas were reported in Volz et al. (2021, figure 3), who used the median as an estimate of the reproductive advantages.

number of new-variant cases is small. The width of the confidence intervals are also influenced by the number of tests that are being sequenced, N_t . For instance, in week 25, this number was relatively small for the simple reason that there were few positive COVID-19 cases in Denmark that week – just 1,315 positive cases of which 1,165 were successfully sequenced. The crude measures for the Alpha variant in the left panel of Figure 3 stabilizes about their average value, 1.73. For the Delta variant, the crude measures are substantially larger and more disperse. The progression of the Delta variant was particularly rapid in weeks 25 and 26.

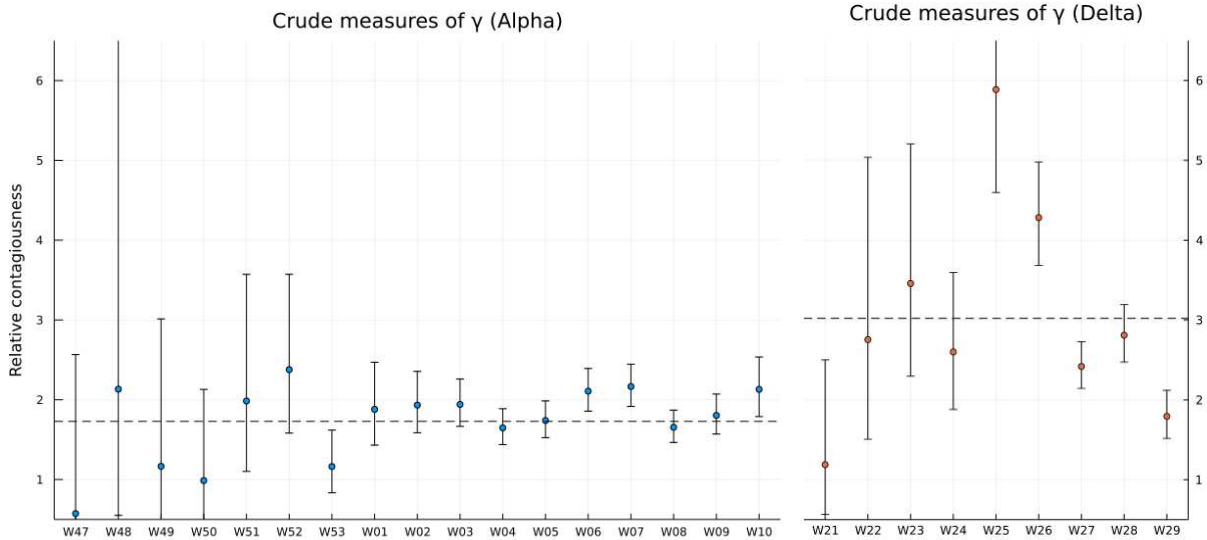


Figure 3: Crude weekly measures of the competitive advantage of the new variant.

The crude measurements of γ in Figure 3 do not fully exploit the information in the data, and the simple sample averages (the dotted lines in Figure 3) do not account for heteroskedasticity and autocorrelation in the measurements errors. To exploit the information in full, we turn to maximum likelihood estimation using the parametrization of the logistic regression. We compute robust standard errors using the Parzen kernel (with bandwidth parameter $K = 4$), see the Appendix. The results are not very sensitive to the choice of bandwidth, but the robust standard errors are somewhat larger than the non-robust standard errors, especially for the Delta variant, see Table A.1.

The maximum likelihood estimates along with 95% confidence intervals are presented in Table 2. The Alpha variant is estimated to be about 86% more contagious per week than the preceding variant, which we refer to as the *ancestral variant*.⁵ The Delta variant, which emerged after then Alpha variant had become completely dominant, is estimated to be 216% more contagious than the Alpha variant on a weekly basis. The reproduction number for SARS-CoV-2 is defined for a generation period (the

⁵The ancestral variant represents a group of variants without a WHO label, with the most prevalent variant before Alpha being B.1.177 also know as 20E (EU1).

Table 2: Empirical estimates for Alpha and Delta.

	Alpha vs Ancestral	Delta vs Alpha	Delta vs Ancestral
<i>Per Week</i>			
α	-7.8 [-9.00,-8.50]	-7.81 [-8.75,-6.87]	
β	0.619 [0.601,0.636]	1.152 [1.026,1.278]	
γ_{week}	1.86 [1.82,1.89]	3.16 [2.79,3.59]	5.87 [5.17,6.67]
<i>Per Generation (4.7 days)</i>			
$\gamma_{4.7\text{days}}$	1.51 [1.50,1.53]	2.17 [1.99,2.36]	3.28 [3.01,3.58]

Note: Empirical estimates with 95% confidence intervals computed with robust standard errors. The estimates of relative contagiousness are $\gamma_{\text{week}} = \exp(\beta)$ and $\gamma_{4.7\text{days}} = \exp(\frac{4.7}{7}\beta)$.

typical time from a person gets infected to the same person infects the next person). For SARS-CoV-2 this period is shorter than a week. Statens Serum Institut in Denmark uses 4.7 days as the generation period, which we adopt in our calculations. We can convert $\hat{\gamma}$ to a period of x days using $\gamma_{x\text{days}} = \exp(\frac{x}{7} \log \gamma_{\text{week}})$, and the estimates for $x = 4.7$ days are presented in the last row of Table 2. The estimates suggest that the Alpha variant has a reproduction number that is about 1.5 times larger than the ancestral variant. The Delta variant is estimated to increase the reproduction number by an additional factor of 2.17, which implies more than a threefold increase relative to the ancestral variant. This is in line with other estimates, which include those for the Alpha variant based on British data by Volz et al. (2021) and those for the Delta variant by Wenseleers (2021). The implication is that it requires a larger proportion $(1 - 1/R_0)$ to be immune to reach *herd immunity*. Suppose that 70% immunity was needed for the ancestral variant. Our estimates of $\gamma_{4.7\text{days}}$ suggest this number increased to about 80% for the Alpha variant and about 90% for the Delta variant.

The estimated model and the observed odds ratios are shown in Figure 4. Overall the model fit looks good, especially for the analysis of the Alpha variant. There are some discrepancies between the data and the linear specification for log odds ratios with the Delta variant. A possible explanation is that many of the COVID-19 cases that were detected in Denmark during the second sample period were contracted abroad. According to the Danish Patient Safety Authority, about 25% of Covid-19 cases were imported cases, primarily by people who had been vacationing in Spain in July.⁶ This could

⁶<https://www.ssi.dk/aktuelt/nyheder/2021/en-stor-del-af-covid-19-smitten-i-danmark-kommer-fra-de-rejsende>

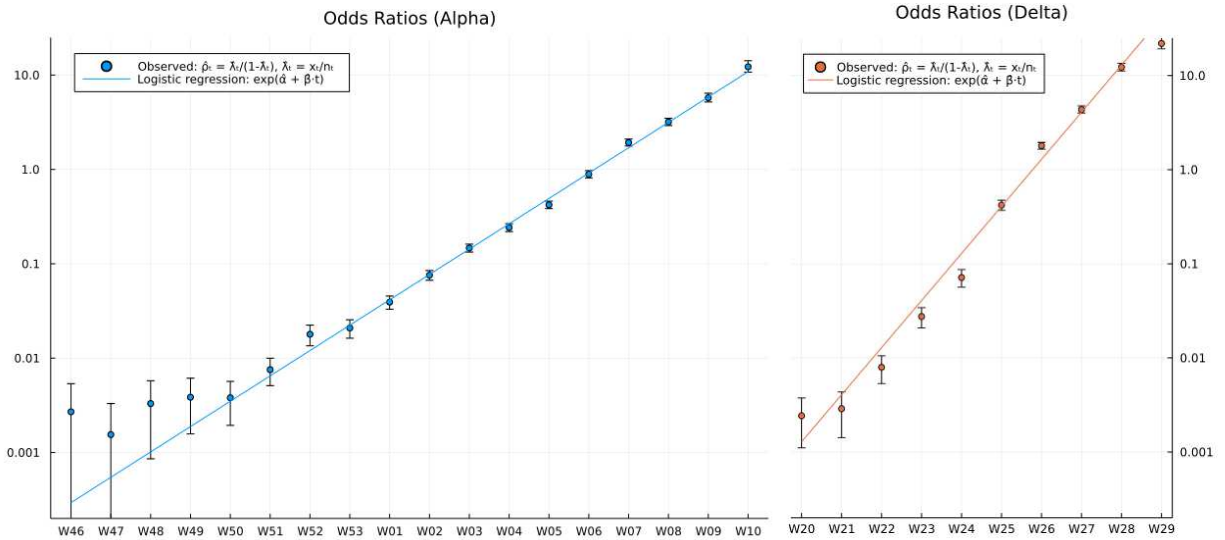


Figure 4: Observed and estimated odds ratios.

potentially influence the progression of the Delta variant because imported cases could be acquired in areas with a higher or a lower Delta proportion than that in Denmark.

A second possible explanation is that the relative contagiousness was different for unvaccinated and vaccinated individuals, causing a gradual shift in the progression of the Delta variant as the vaccine coverage increased. A study based on breakthrough infections in Denmark during the period from March 1, 2021 to August 3, 2021 found a small decline in vaccine effectiveness against the Delta variant. The Pfizer vaccine was reported to be 81.0% (95% CI: 79.4; 82.4) effective at preventing Alpha variant infections and 78.8% (95% CI: 77.2; 80.4) effective at preventing Delta variant infections.⁷ The Pfizer vaccine (Comirnaty) is the most commonly used vaccine in Denmark and accounts for about 85% of all vaccinations. The study only reported vaccine efficacy for fully vaccinated individuals, which only accounted for a small percentage of individuals during this period. A large discrepancy in efficacy between the Alpha and Delta variants following a single vaccine dose could potentially have influenced our analysis. However, the right panel of Figure 4 does not suggest a gradual change in the slope but a minor parallel shift around Week 25.

A third possible explanation is that restrictions were largely abolished during the second sample period, which could result in more noisy data for the Delta variant and possible misspecification of the model. During the Alpha sample period restrictions were quite restrictive. In contrast, during the Delta sample period most restrictions were abolished in Denmark, especially in relation to large gatherings. The relaxed restrictions may explain the larger degree of randomness in the progression of the Delta

⁷<https://www.ssi.dk/aktuelt/nyheder/2021/der-er-fortsat-hoj-vaccineeffektivitet-for-covid-19-vaccinerne>

variant. For instance, the Euro 2020 games in Copenhagen may have contributed to the accelerated growth in the Delta variant in Week 25 (see right panel of Figure 4) because spectators at two games accounted for a large fraction of the Delta variant cases. Following the Denmark-Belgium Euro 2020 game in Copenhagen on June 17, 2021, 41 attending spectators tested positive for COVID-19 of which 25 cases (61.0%) were the Delta variant. The following week, on Monday June 21, 2021, Denmark played Russia in Copenhagen at another Euro 2020 game, where 62 cases were subsequently detected among spectators of which 28 (45.2%) were Delta variant cases. These are large numbers and percentages, because the total number of Delta variant cases in Week 24 and Week 25 were 91 and 345, respectively, and Delta variant only accounted for 6.7% in Week 24 and 29.6% in Week 25. The binomial model for Delta variant cases, assumes that the individual cases are generated by independent Bernoulli random variables. This independence assumption becomes questionable when a large proportion of cases can be linked to the same events. The right panel of Figure 4 is consistent with a single larger than expected jump in the proportion of Delta cases around the time of the Euro 2020 games, and two parallel lines (one fitting data up until Week 24 and one fitting data from Week 25 and onwards) would appear to fit the data about as well as a single line can fit the data in the left panel of Figure 4.

3.2 Omicron Variant

A earlier version of this paper, dated November 7, 2021, analyzed the Alpha and Delta variants and concluded: “It is unclear when a more contagious variant will emerge, if at all”. This was resolved unequivocally a few weeks later with the arrival of the Omicron variant. Below we analyze the competitive advantage of the Omicron variant and we will use daily data because this variant progressed to become dominant even faster than earlier variants.

Several notable changes occurred during the period where Omicron emerged. With the emergence of Omicron along with a rapid increase in COVID-19 case numbers, the Danish health authorities rapidly expanded the booster vaccination program (3rd dose of an mRNA vaccine) and recommended several preventive measures to slow the spread of the virus. In December alone, 1,960,421 individuals received a COVID-19 booster vaccine, which was in addition to 847,187 individuals who had received the booster vaccine before December 1, 2021.⁸ Effective December 10th, mask requirements were reintroduced along with new restrictions on nightlife, restaurants, and indoor gatherings. Moreover, school children went back to remote learning on December 15th.

The daily data for December 2021 are given in Table 3. Nearly 6 million COVID-19 PCR tests⁹

⁸Source: SSI. <https://covid19.ssi.dk/overvagningsdata/download-fil-med-vaccinationsdata>

⁹An additional 6.8 million antigen tests were performed during the same months. A positive antigen test is usually

Table 3: Daily COVID-19 PCR tests and outcomes (Omicron)

Date	Tested (PCR)	Cases C_t	Sequenced (successfully)		Omicron	Omicron
			N_t	(N_t/C_t)	cases X_t	proportion X_t/N_t
2021-12-01	185,372	4,910	4,267	(86.9%)	77	1.8%
2021-12-02	213,494	5,040	4,294	(85.2%)	62	1.4%
2021-12-03	188,041	5,651	4,946	(87.5%)	75	1.5%
2021-12-04	140,790	5,577	5,089	(91.2%)	111	2.2%
2021-12-05	147,722	5,450	4,995	(91.7%)	167	3.3%
2021-12-06	209,434	7,645	6,762	(88.4%)	337	5.0%
2021-12-07	207,987	7,902	6,928	(87.7%)	515	7.4%
2021-12-08	205,263	7,136	6,232	(87.3%)	649	10.4%
2021-12-09	243,089	7,157	6,228	(87.0%)	707	11.4%
2021-12-10	210,756	7,520	6,444	(85.7%)	843	13.1%
2021-12-11	153,995	7,210	6,443	(89.4%)	1,080	16.8%
2021-12-12	165,474	7,723	6,794	(88.0%)	1,521	22.4%
2021-12-13	229,948	11,350	9,316	(82.1%)	2,691	28.9%
2021-12-14	221,944	12,252	10,456	(85.3%)	4,044	38.7%
2021-12-15	217,007	12,041	10,409	(86.4%)	4,827	46.4%
2021-12-16	254,680	11,388	9,475	(83.2%)	4,438	46.8%
2021-12-17	233,617	11,950	9,860	(82.5%)	5,213	52.9%
2021-12-18	174,168	11,420	9,233	(80.8%)	5,163	55.9%
2021-12-19	180,302	11,717	7,927	(67.7%)	4,908	61.9%
2021-12-20	267,264	15,228	2,565	(16.8%)	1,611	62.8%
2021-12-21	254,893	14,875	3,199	(21.5%)	2,437	76.2%
2021-12-22	269,139	13,684	1,323	(9.7%)	1,035	78.2%
2021-12-23	243,139	14,729	3,450	(23.4%)	2,708	78.5%
2021-12-24	71,463	8,322	597	(7.2%)	494	82.7%
2021-12-25	71,502	9,233	915	(9.9%)	705	77.0%
2021-12-26	79,592	12,300	2,297	(18.7%)	1,986	86.5%
2021-12-27	182,893	25,168	4,657	(18.5%)	4,134	88.8%
2021-12-28	191,226	24,273	1,471	(6.1%)	1,324	90.0%
2021-12-29	213,584	19,292	359	(1.9%)	333	92.8%
2021-12-30	225,529	21,727	910	(4.2%)	829	91.1%
2021-12-31	71,125	11,027	429	(3.9%)	393	91.6%

Note: Source is *Variant-PCR svar fra 27. nov. og frem, Testcenter Danmark* SSI, January 16, 2022. Data available at: <https://files.ssi.dk/covid19/podepind-sekventering/variant-pcr-test-december2021/opgoerelse-variantpcr-covid19-16012022-q9zx>

were performed during the month of December and the variant was determined in 158,270 of 350,897 positive test. Initially SSI attempted to sequence nearly all positive tests, but was unable to keep up with many cases and began sequencing a representative sample in late December.¹⁰ The Omicron

¹⁰It is unclear how the representative sampling is conducted and whether it is properly stratified by region, age, and vaccination status. SSI states: "The proportion of Omicron cases is calculated using only omicron variant PCR tested

proportion grew from 10.4% on December 8th to 90% on December 28th and COVID-19 cases more than tripled in this period.

The maximum likelihood estimates along with 95% confidence intervals are presented in Table 4.¹¹ Just prior to the emergence of Omicron, the Delta variant accounted for virtually all COVID-19 cases in Denmark. The estimates can therefore be interpreted as the competitive advantage of Omicron relative to Delta in a population where about 80% are fully vaccinated. The latter has important implications for the external validity of these empirical results. The competitive advantages estimated for Alpha and Delta can be translated to larger basic reproduction numbers, because these variants emerged in a population with little prior immunity. In contrast, Omicron emerged in populations with a high degree of prior immunity from vaccinations and prior infections, and Omicron’s ability to evade prior immunity explains a large part its competitive advantage over Delta. It is therefore not clear (from these data alone) if the basic reproduction number is substantially larger for Omicron than for Delta. The competitive advantage of Omicron could therefore vary across population with different degrees of prior immunity and between regions with different restrictions. In the Danish population with high vaccine coverage, Omicron is estimated to be 28% more competitive than Delta *per day*, which translate to 5.5 times more competitive per week. For the sake of comparison, we also report the competitive advantage of the Omicron variant *per 4.7 days*, although the generation time for Omicron may be shorter than that of Delta. This estimate is in line with Nishiura et al. (2022), who also noted that the increase in the basic reproduction number (for Omicron relative to Delta) “is likely very small, e.g. in the order of 10-20%”.

Table 4: Empirical estimates for Omicron (vs Delta).

	α	β	γ
<i>Per Day</i>	-4.11 [-4.49,-3.74]	0.244 [0.221,0.267]	1.28 [1.25,1.31]
<i>Per Generation (4.7days)</i>			3.15 [2.83,3.50]
<i>Per Week</i>			5.52 [4.70,6.47]

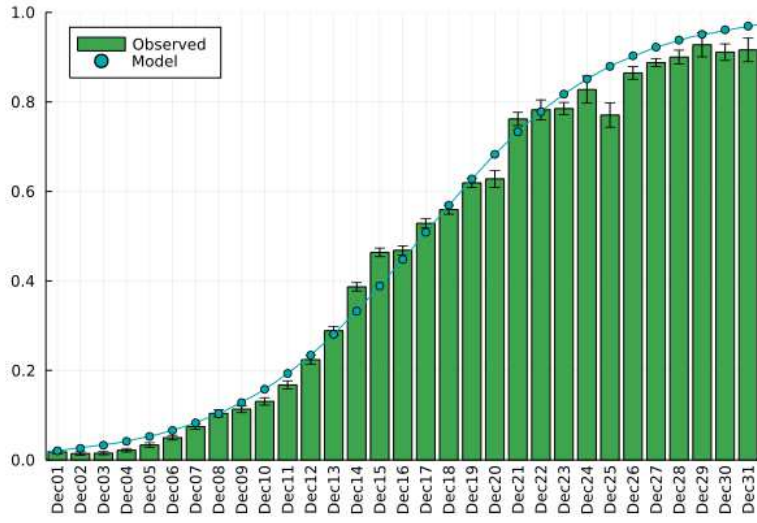
Note: Empirical estimates with 95% confidence intervals computed with robust standard errors.

samples from Test Center Denmark. We expect that the calculated proportion is representative for all the confirmed SARS-CoV-2 cases."

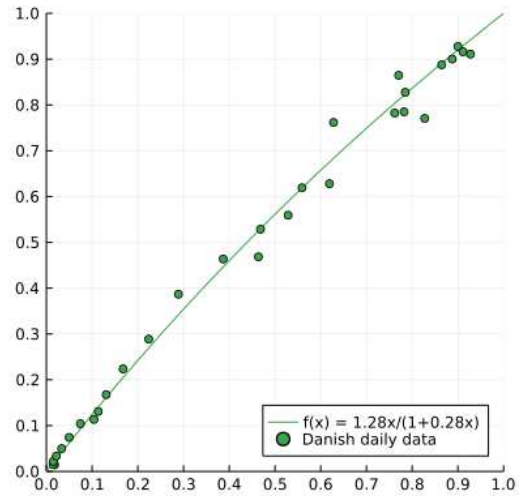
¹¹The robust standard errors are computed with the Parzen kernel and bandwidth parameter $K = 4$, as was the case in the analysis of the Alpha and Delta variants.

The four panels of Figure 5 present results for Omicron that are analogous to the results presented for Alpha and Delta in Figures 1-4. Panel (a) displays the daily proportion of Omicron in positive PCR tests that were successfully sequenced and the solid line is the proportion implied by the estimated model. The model tracks the observed proportions reasonably well with the exception of the last week where it overpredicts the proportion of Omicron. Below, we discuss possible explanations for this and other discrepancies. Panel (b) in Figure 5 shows the daily progression implied by a daily competitive advantage of $\gamma = 1.28$. The crude measures in Panel (c) are more erratic than the crude measures based on the weekly data in Figure 3. The dashed line represents their average value, which (at 1.27) is close to the maximum likelihood estimate. Panel (d) displays the estimated model for the daily odds ratios, ρ_t , and the observed odds ratios. The estimate of γ defines the slope of the fitted line in Panel (d). The observed data suggests some time variation in γ , including weekly periodicity, which can also be seen in Panel (c). Many of the Omicron cases in early December were traced to super spreader events, which had occurred during weekend activities and it is interesting to note that the odds ratios for Omicron tend to be relatively large on Wednesdays (December 1, 8, 15, 22, and 29), because Wednesdays are days where individuals infected during the weekend are likely to test positive. The periodic variation across day-of-the-week may be explained by Omicron having a particular competitive advantage during events that tend to occur during weekends. Another possible explanation is that Omicron was more prevalent among young adults, and these age cohorts accounted for a disproportional large share of infections that were detected on Wednesdays. More detailed data where case numbers are stratified by both variant and age could cast light on this aspect.

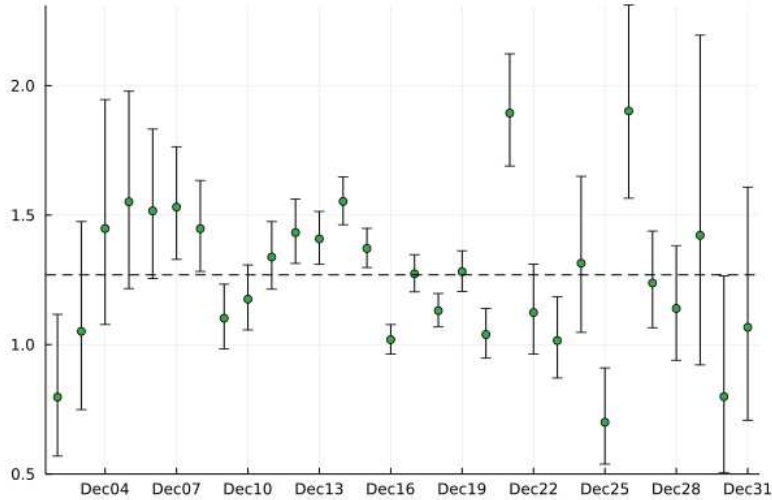
The progression of Omicron is below the estimated trendline towards the end of December. The possible explanations for this are many. First, the Christmas holiday may have played a role, for instance by changing contact patterns and increased use of preventive testing before seeing relatives. Second, it is also possible that the sampling of positive PCR tests, which was adopted in late December, did not succeed in being representative. Third, it is also possible that restrictions introduced in mid December were relatively more effective at preventing Omicron transmissions than Delta transmissions. A fourth possible explanation is that booster vaccinations induced time variation in γ . There was a large shift in population immunity during the month of December, as a large share of the population received a booster vaccine. The competitive advantage of Omicron might be smaller in this subpopulation and this is supported by the evidence that boosters vaccination greatly reduce the risk of Omicron infections, see Lyngse et al. (2022), and the observation that the percentage of Omicron cases increased in the unvaccinated group during the month of December. It would be interesting to generalize the



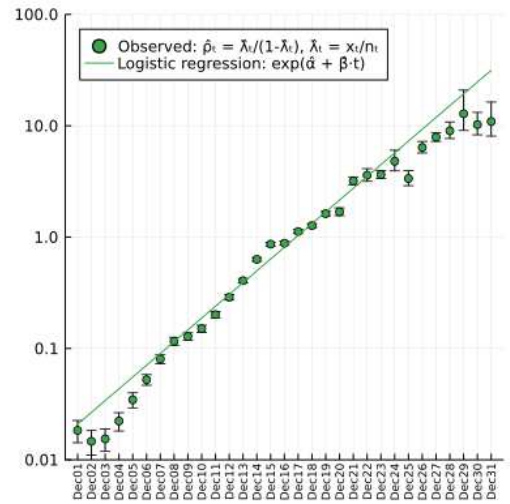
(a) Daily proportion of Omicron



(b) Daily Progression of Omicron



(c) Crude Measures



(d) Daily Odds Ratios

Figure 5: Figures with empirical results for the Omicron variant.

model framework to encompass subpopulations with different values of γ . This would require a careful modeling of the interactions between groups and data with the required granularity.

4 Confidence Intervals, Predictions, and Inferring reproduction Number

In this section, we detail two ancillary results. First, in Section 4.1, we show the estimated model can be used to predict the proportion of an emerging virus variant and develop methods for quantifying the associated uncertainty. We illustrate these methods with the data for the Alpha variant. Then, in Section 4.2, we develop a simple formula for the reproduction number of the new variant, which does not require concurrent genome data. Instead it projects the most recent estimate of the proportion forward and infer the effective reproduction number from the recent growth in total cases.

4.1 Confidence Sets and Out-of-Sample Analysis

At times T we can estimate α and β , as well as their variance-covariance matrix, $\Sigma_T = \text{var}((\hat{\alpha}_T, \hat{\beta}_T)')$, where $\hat{\alpha}_T$, $\hat{\beta}_T$, and $\hat{\Sigma}_T$ denote the resulting estimates. Point forecasts for the proportion of the new virus variant, λ_t , are given from (2). The h period ahead point forecast, made at time T , is simply

$$\hat{\lambda}_{T+h,T} = 1 / \left[1 + \exp\{-\hat{\alpha}_T - \hat{\beta}_T(T+h)\} \right],$$

and the corresponding confidence bands can be deduced from the asymptotic distribution of $(\hat{\alpha}_T, \hat{\beta}_T)$. The confidence band based on c units of standard deviations is given by

$$1 / \left[1 + \exp\{-\hat{\alpha}_T - \hat{\beta}_T(T+h) \pm c\sqrt{v(T+h, \hat{\Sigma}_T)}\} \right], \quad (3)$$

where $c = 1.96$ would correspond to a 95% confidence bands and

$$v(T+h, \hat{\Sigma}_T) \equiv \hat{\text{var}}(\hat{\alpha}_T + \hat{\beta}_T(T+h)) = (1, T+h)\hat{\Sigma}_T(1, T+h)'$$

The estimated and predicted progression of λ_t for the Alpha variant along with confidence bands (using $c = 2$ and $c = 4$ standard deviations) are presented in Figure 6. The saltires (x-crosses) in Figure 6 are the observed weekly empirical proportion of the Alpha variant.

In the upper left panel of Figure 6, we have estimated the model by maximum likelihood using 4

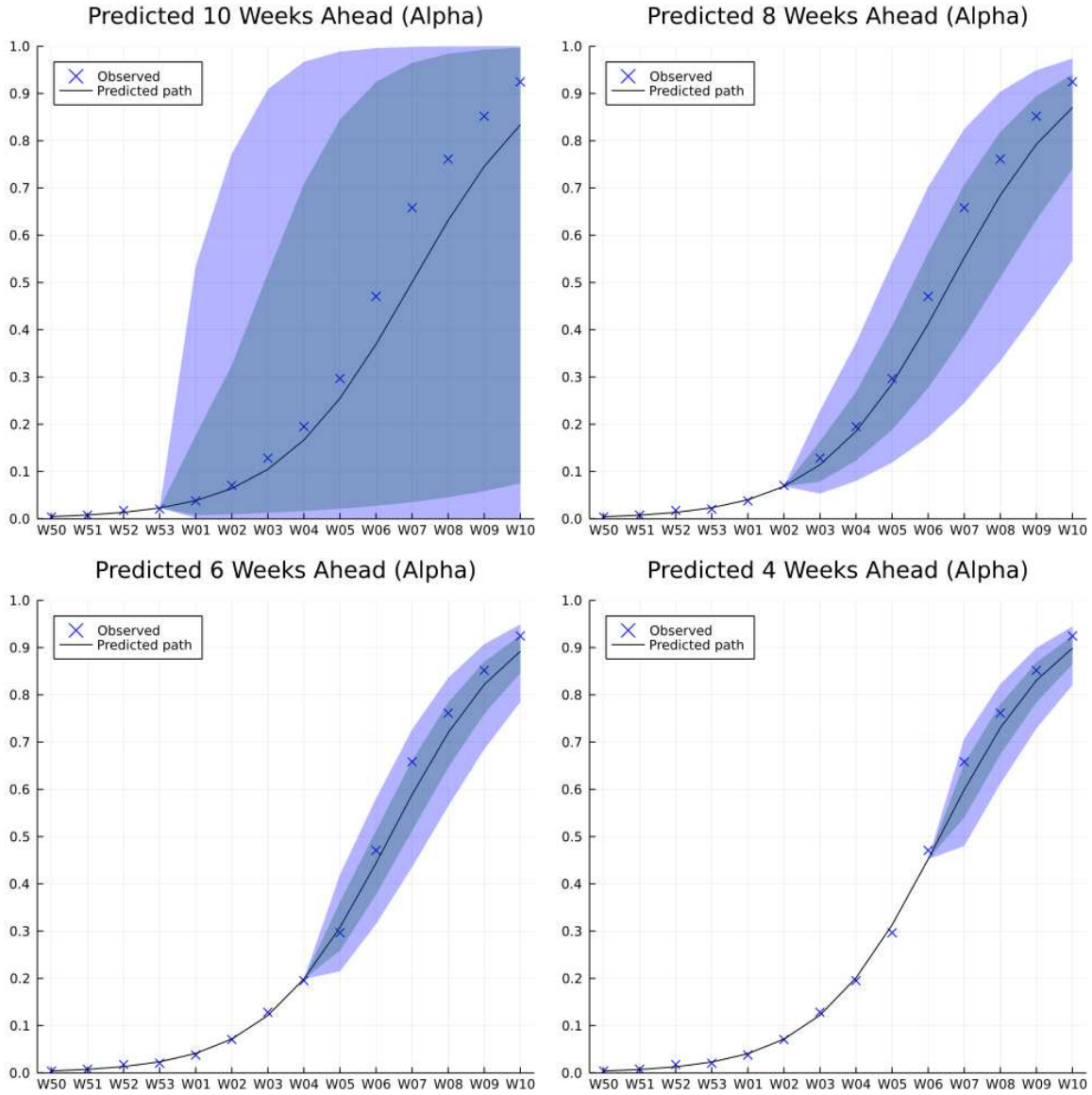


Figure 6: The predicted path for λ_t (solid black line) is shown for when the model is estimated with, 4, 6, 8, and 10 weeks of data, which translates to an out-of-sample period of 10, 8, 6 and 4 weeks, respectively. The shaded areas are the confidence bands using $2\times$ and $4\times$ the standard deviation as defined in (3). The observed proportion of Alpha are indicated with the blue crosses.

weeks of data (Week 50-53) which leaves 10 weeks for out-of-sample forecasting. The point forecasts are reasonably close to the realized proportions, but with just four weeks of data for estimation, there is a great deal of uncertainty about the estimated parameters, causing $v(T+h, \hat{\Sigma}_T)$ to be large. With two additional weeks for estimation (six weeks total), the parameters are more precisely estimated, resulting in tighter confidence bands, as shown in the upper-right panel of Figure 6. With eight or ten weeks for estimation, the parameter estimates become even more accurate, resulting in the even tighter confidence intervals in the two lower panels. The point forecasts are reasonably accurate at horizons up to four weeks, but tend to be below the realized values, especially at longer horizons. This is because the four in-sample estimates of γ ($\hat{\gamma}_{W53} = 1.71$, $\hat{\gamma}_{W02} = 1.76$, $\hat{\gamma}_{W04} = 1.79$, and $\hat{\gamma}_{W06} = 1.81$) are all smaller than the full sample estimate: $\hat{\gamma} = 1.86$. This highlights that we should expect the out-of-sample forecasting errors to be positively autocorrelated and likely have the same sign as $\gamma - \hat{\gamma}_T$. It should be noted that the confidence bands reflect the uncertainty about λ_{T+h} , while the realized empirical proportions, X_{T+h}/N_{T+h} , are themselves noisy estimates of λ_{T+h} , see the confidence bands in Figure 1.

4.2 Inferring the Reproduction Number for the New Variant in Real Time

We can infer the effective reproduction number for an emerging variant from the effective reproduction number of all cases when combined with knowledge about λ and γ . Let C be the number of all cases in this period, of which $B = \lambda C$ are the new-variant cases and $A = (1 - \lambda)C$ are the old-variant cases. If the current reproduction number for all cases is R , then there were C/R cases one generation ago. Similarly, there were $B/R_B = \lambda C/R_B$ new-variant cases and $A/R_A = (1 - \lambda)C/R_A$ old-variant cases one generation earlier, where R_A and R_B denote the current reproduction numbers for the old and new variant, respectively. The number of cases for the previous generation have to add up to the total number of cases. Hence, $C/R = \lambda C/R_B + (1 - \lambda)C/R_A$, and since $R_A = R_B/\gamma$ it follows that

$$R_B = R_B(\lambda, R, \gamma) = R[\lambda + \gamma(1 - \lambda)]. \quad (4)$$

The value of λ to be used in this expression should be the that for the current period, which is typically predicted from earlier periods, and the value of γ to be used in (4), should be the one that corresponds to the same generation period as used to compute R . We estimated $\gamma_{4.7\text{days}} \approx 1.5$ for the Alpha variant and $\gamma_{4.7\text{days}} \approx 2$ for Delta. Thus, based on the Danish data we approximately have,

$$R_{\text{Alpha},T} \approx R_T \times (1.5 - 0.5\lambda_T) \quad \text{and} \quad R_{\text{Delta},T} \approx R_T \times (2 - \lambda_T).$$

This formula makes it possible to assess the reproduction number for an emerging variant before concurrent sequencing data are available. The reproduction number, R_T , for all cases can be inferred from the progression in the total number of COVID-19 cases and the proportion of the new variant, λ_T , can be obtained from the estimated model, by projecting forward the most recent knowledge about the proportion, see Figure 4.

4.2.1 Empirical Illustration for the Alpha Variant

We can use (4) to characterize the combinations of (λ, R) that correspond to a particular reproduction number for the Alpha variant. A contour plot for $R_B(\lambda, R)$ based on the point estimate of γ that corresponds to a generation period, $\hat{\gamma}_{4.7\text{days}} = \exp(\frac{4.7}{7} \log \hat{\gamma})$, is presented in Figure 7. The region above the solid line, $\{(\lambda, c) : R_B(\lambda, R, \hat{\gamma}_{4.7\text{days}}) > 1\}$, are the combinations of λ and R where case numbers for Alpha are increasing, and the region below the solid line is the region where Alpha cases are decreasing. The shaded region about the solid line represent the uncertainty about the threshold, due to uncertainty about γ . The shaded area is given by

$$\{(\lambda, R) : R_B(\lambda, R, \gamma) = 1, \text{ for some } \gamma \in \text{CI}_{95\%}\},$$

where $\text{CI}_{95\%}$ is the 95% confidence interval for $\hat{\gamma}_{4.7\text{days}}$ we obtained in Section 3. Note that the uncertainty interval shrinks to zero as $\lambda \rightarrow 1$. The reason is that the limited case, $\lambda = 1$, represents the situation where Alpha cases make up all cases, and its rate of increase can therefore be inferred from the rate of increase in all cases. More formally, the result follows from the fact that $R_B/R = \lambda + \gamma(1 - \lambda) \rightarrow 1$ as $\lambda \rightarrow 1$.

A model-free proxy for λ_t is X_t/N_t and a crude estimate of R in week t , is given by $\hat{R}_t \equiv \exp(\frac{4.7}{7} \log \frac{\text{Cases}_t^{\text{Adj}}}{\text{Cases}_{t-1}^{\text{Adj}}})$, where $\text{Cases}_t^{\text{Adj}}$ is the number of all cases in week t after adjusting for the testing intensity. The adjustment is given by $\text{Cases}_t^{\text{Adj}} = \text{Cases}_t \times \left(\frac{\text{Tested}_t}{M}\right)^{-0.7}$, where M is a baseline number of tests, see Statens Serum Institut (2020). The baseline number, M , does not influence the ratio because,

$$\frac{\text{Cases}_t^{\text{Adj}}}{\text{Cases}_{t-1}^{\text{Adj}}} = \frac{\text{Cases}_t}{\text{Cases}_{t-1}} \times \left(\frac{\text{Tested}_t}{\text{Tested}_{t-1}}\right)^{-0.7},$$

and we use this ratio to compute \hat{R}_t .

The estimated reproduction number, \hat{R}_t , is plotted against the observed proportion of the Alpha variant in Figure 7, labelled with the corresponding week number. All pairs fall above the solid line, where the effective reproduction number for the Alpha variant is greater than one. This indicates that

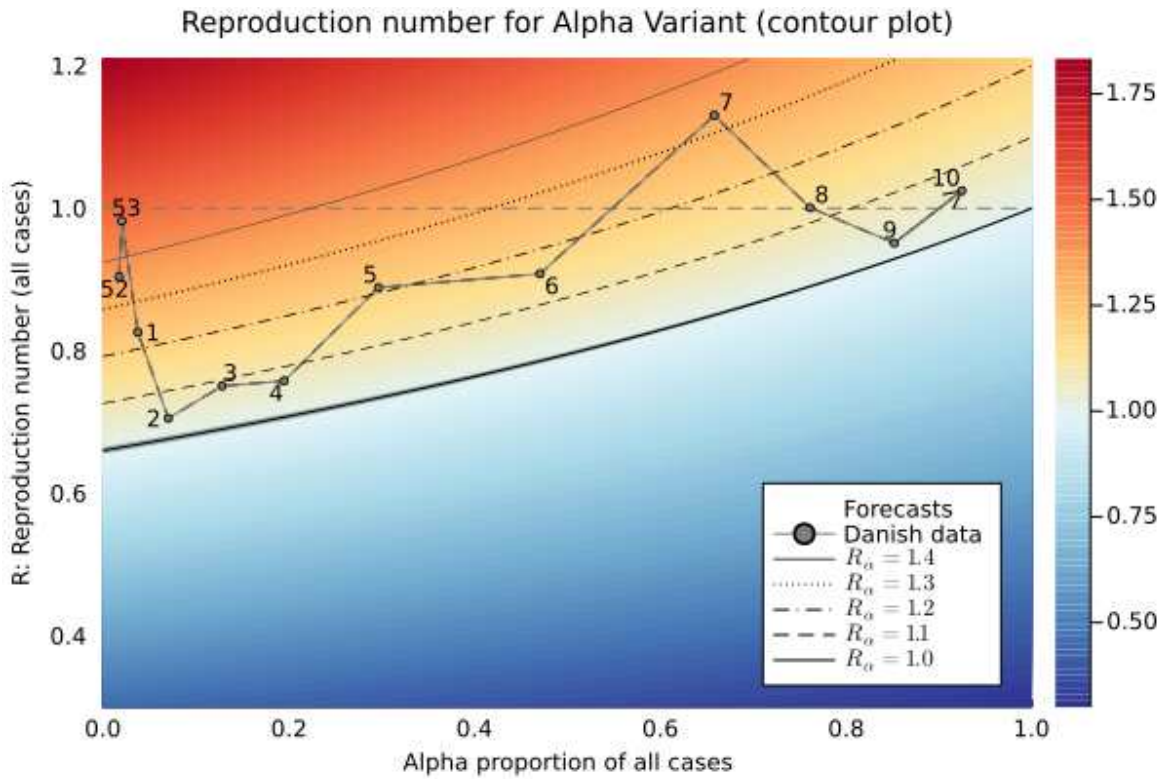


Figure 7: Contour plot of weekly reproduction numbers for Alpha.

the number of Alpha cases (detected and undetected) was growing throughout the sample period even though the total number of cases was declining most weeks in this sample period.

5 Discussion

We have shown how the relative contagiousness of a new virus variant can be estimated by maximum likelihood and how robust standard errors can be computed. The underlying structure is that of a logistic regression model. We applied the methodology to Danish data from the periods where the Alpha, Delta, and Omicron variants emerge and become dominant. The methodology can also be applied to data with irregular sampling frequencies, such as time series with missing data, and the analysis can be extended to situations with more than two competing variants as detailed in Appendix A. The framework is not specific to the analysis of competing virus variant, but can be applied in a context with other competing objects. We found the Alpha variant increased the contagiousness by about 50% and the Delta variant increased the contagiousness further by more than 100% per generation. We estimated the Omicron variant to be about three times more infectious than the Delta variant in a highly vaccinated population. The empirical results should be interpreted in relation to

the data they were estimated with. The results for Alpha and Delta were derived in a population that was largely immune naive. These findings have external validity, because they relates directly to the basic reproduction number of the virus. The results for Omicron do not have the same degree of external validity because the competitive advantage was estimated in a population with a particular (and changing) composition of immunity.

Three new variants of the SARS-CoV-2 have emerged to become dominant in short succession. There were just 18 weeks between the time the Alpha variant made up 90% of all cases in Denmark to the time the Delta variant surpassed that same threshold, and 28 weeks later the Omicron variant accounted for over 90% of all cases. It is therefore reasonable to expect that even more contagious variants will emerge in the time to come. While the first two variants were not only more contagious but also found to increase the risk of hospitalization. Fortunately, there is evidence that the Omicron variant is less severe and despite the many breakthrough infections there is strong evidence that vaccinations continue to abate transmissions and greatly reduce the risk of severe disease.

References

- A. Rambaut, N. Loman, O. Pybus, W. Barclay, J. Barrett, A. Carabelli, T. Connor, T. Peacock, D. L. Robertson, E. Volz, Preliminary genomic characterisation of an emergent SARS-CoV-2 lineage in the UK defined by a novel set of spike mutations, 2020.
- E. Volz, S. Mishra, M. Chand, J. C. Barrett, R. Johnson, L. Geidelberg, W. R. Hinsley, D. J. Laydon, G. Dabrera, Á. O’Toole, R. Amato, M. Ragonnet-Cronin, I. Harrison, B. Jackson, C. V. Ariani, O. Boyd, N. J. Loman, J. T. McCrone, S. Gonçalves, D. Jorgensen, R. Myers, V. Hill, D. K. Jackson, K. Gaythorpe, N. Groves, J. Sillitoe, D. P. Kwiatkowski, S. Flaxman, O. Ratmann, S. Bhatt, S. Hopkins, A. Gandy, A. Rambaut, N. M. Ferguson, Transmission of SARS-CoV-2 lineage B.1.1.7 in England: Insights from linking epidemiological and genetic data, medRxiv (2021). URL: <https://www.medrxiv.org/content/early/2021/01/04/2020.12.30.20249034.1>. doi:10.1101/2020.12.30.20249034. arXiv:<https://www.medrxiv.org/content/early/2021/01/04/2020.12.30.20249034.1.full.pdf>.
- N. L. Washington, K. Gangavarapu, M. Zeller, A. Bolze, E. T. Cirulli, K. M. Schiabor Barrett, B. B. Larsen, C. Anderson, S. White, T. Cassens, S. Jacobs, G. Levan, J. Nguyen, J. M. Ramirez, C. Rivera-Garcia, E. Sandoval, X. Wang, D. Wong, E. Spencer, R. Robles-Sikisaka, E. Kurzban, L. D. Hughes, X. Deng, C. Wang, V. Servellita, H. Valentine, P. De Hoff, P. Seaver, S. Sathe, K. Gietzen, B. Sickler, J. Antico, K. Hoon, J. Liu, A. Harding, O. Bakhtar, T. Basler, B. Austin, M. Isaksson, P. Febbo, D. Becker, M. Laurent, E. McDonald, G. W. Yeo, R. Knight, L. C. Laurent, E. de Feo, M. Worobey, C. Chiu, M. A. Suchard, J. T. Lu, W. Lee, K. G. Andersen, Genomic epidemiology identifies emergence and rapid transmission of SARS-CoV-2 B.1.1.7 in the United States, medRxiv (2021). URL: <https://www.medrxiv.org/content/early/2021/02/07/2021.02.06.21251159>. doi:10.1101/2021.02.06.21251159. arXiv:<https://www.medrxiv.org/content/early/2021/02/07/2021.02.06.21251159.full.pdf>.

- P. Bager, J. Wohlfahrt, J. Fonager, M. Albertsen, T. Yssing Michaelsen, C. H. Møller, S. Ethelberg, R. Legarth, M. S. Fischer Button, S. M. Gubbels, M. Voldstedlund, K. Mølbak, R. L. Skov, A. Fomsgaard, T. Grove Krause, The Danish Covid-19 Genome Consortium, Increased risk of hospitalisation associated with infection with SARS-CoV-2 lineage B.1.1.7 in Denmark, *Lancet* 21 (2021) 1351. doi:[https://doi.org/10.1016/S1473-3099\(21\)00290-5](https://doi.org/10.1016/S1473-3099(21)00290-5).
- R. Viana, S. Moyo, D. G. Amoako, H. Tegally, C. Scheepers, C. L. Althaus, U. J. Anyaneji, P. A. Bester, M. F. Boni, M. Chand, W. T. Choga, R. Colquhoun, M. Davids, K. Deforche, D. Doolabh, L. du Plessis, S. Engelbrecht, J. Everatt, J. Giandhari, M. Giovanetti, D. Hardie, V. Hill, N.-Y. Hsiao, A. Iranzadeh, A. Ismail, C. Joseph, R. Joseph, L. Koopile, S. L. K. Pond, M. U. G. Kraemer, L. Kuate-Lere, O. Laguda-Akingba, O. Lesetedi-Mafoko, R. J. Lessells, S. Lockman, A. G. Lucaci, A. Maharaj, B. Mahlangu, T. Maponga, K. Mahlakwane, Z. Makatini, G. Marais, D. Maruapula, K. Masupu, M. Matshaba, S. Mayaphi, N. Mbhele, M. B. Mbulawa, A. Mendes, K. Mlisana, A. Mnguni, T. Mohale, M. Moir, K. Moruisi, M. Mosepele, G. Motsatsi, M. S. Motswaledi, T. Mphoyakgosi, N. Msomi, P. N. Mwangi, Y. Naidoo, N. Ntuli, M. Nyaga, L. Olubayo, S. Pillay, B. Radibe, Y. Ramphal, U. Ramphal, J. E. San, L. Scott, R. Shapiro, L. Singh, P. Smith-Lawrence, W. Stevens, A. Strydom, K. Subramoney, N. Tebeila, D. Tshiabuila, J. Tsui, S. van Wyk, S. Weaver, C. K. Wibmer, E. Wilkinson, N. Wolter, A. E. Zarebski, B. Zuze, D. Goedhals, W. Preiser, F. Treurnicht, M. Venter, C. Williamson, O. G. Pybus, J. Bhiman, A. Glass, D. P. Martin, A. Rambaut, S. Gaseitsiwe, A. von Gottberg, T. de Oliveira, Rapid epidemic expansion of the SARS-CoV-2 Omicron variant in southern Africa, *Nature* (2022) forthcoming.
- H. White, *Estimation, Inference and Specification Analysis*, Cambridge University Press, Cambridge, 1994.
- M. Besançon, D. Anthoff, A. Arslan, S. Byrne, D. Lin, T. Papamarkou, J. Pearson, *Distributions.jl: Definition and modeling of probability distributions in the JuliaStats ecosystem*, arXiv e-prints (2019) arXiv:1907.08611. arXiv:1907.08611.
- D. Lin, S. Byrne, J. M. White, A. Noack, M. Besançon, D. Bates, D. Widmann, J. Pearson, J. Zito, A. Arslan, K. Squire, M. Schauer, D. Anthoff, T. Papamarkou, J. Drugowitsch, B. Deonovic, A. Sengupta, G. Ragusa, G. Moynihan, B. J. Smith, M. O’Leary, Michael, M. J. Innes, C. Dann, G. Lacerda, I. Dunning, J. Chen, M. Tarek, T. K. Papp, *JuliaStats/Distributions.jl: v0.25.11*, 2021. URL: <https://doi.org/10.5281/zenodo.5105997>. doi:10.5281/zenodo.5105997.
- R Core Team, *R: A Language and Environment for Statistical Computing*, R Foundation for Statistical Computing, Vienna, Austria, 2018. URL: <https://www.R-project.org>.
- P. R. Hansen, Replication files for ‘relative contagiousness of emerging virus variants: An analysis of the Alpha, Delta, and Omicron SARS-CoV-2 variants’ URL:github.com/reinhardhansen/VirusVariantsReplicationFiles (2022).
- T. Wenseleers, Analysis of the growth rate advantage and increase in infectiousness of the SARS-Cov2 variant of concern B.1.617.2, also know as the Delta variant, in India and selected other countries URL:github.com/tomwenseleers/covid-delta (2021).
- H. Nishiura, K. Ito, A. Anzai, T. Kobayashi, C. Piantham, A. J. Rodriguez-Morales, Relative reproduction number of SARS-CoV-2 Omicron (B.1.1.529) compared with Delta variant in South Africa, *Journal of Clinical Medicine* 11 (2022) 30.

F. P. Lyngse, K. Mølbak, M. Denwood, L. E. Christiansen, C. H. Møller, M. Rasmussen, A. S. Cohen, M. Stegger, J. Fonager, R. Sieber, K. Ellegaard, C. Nielsen, C. T. Kirkeby, Effect of vaccination on household transmission of SARS-CoV-2 Delta VOC, medRxiv (2022). URL: <https://www.medrxiv.org/content/early/2022/01/06/2022.01.06.22268841>. doi:10.1101/2022.01.06.22268841.

Statens Serum Institut, Ekspertreport af d. 23. oktober 2020: Incidens og fremskrivning af COVID-19 tilfælde, 2020.

J. Revels, M. Lubin, T. Papamarkou, Forward-mode automatic differentiation in Julia, arXiv:1607.07892 [cs.MS] (2016). URL: <https://arxiv.org/abs/1607.07892>.

Appendix A: The Case with Multiple Competing Virus Variants

In this Appendix we consider the model extension to the case where there may be more than two competing virus variant. Although this was not relevant in the analysis of the Danish data, other countries have reported a sizable proportion of three or more variants simultaneously. For instance, France had four variants that each accounted for more than 5% of all COVID-19 cases in the second half of June, 2021, Delta (41%), Alpha (29%), Beta (19%), and Gamma (7%).¹²

For $j = 1, \dots, m$, we let $C_{j,t}$ and $\lambda_{j,t} = C_{j,t}/C_t$ denote the number of cases and the proportion of the j -th variant at time t . Here m is the number of virus variants and $C_t = \sum_{j=1}^m C_{j,t}$ is the total number of cases at time t . We measure the contagiousness of all variants relative to the first variant ($j = 1$) and let $a_{t+1} = C_{1,t+1}/C_{1,t}$ represent the progression in this variant. So, the first variant is used as the numeraire and the relative contagiousness of other variants is represented by the parameter, γ_j , $j = 1, \dots, m$ with $\gamma_1 = 1$. Analogous to the case with two variants we now have

$$C_{j,t+1} = \gamma_j a_{t+1} C_{j,t}, \quad j = 1, \dots, m,$$

and the evolution of the variant proportions are given by

$$\begin{aligned} \lambda_{j,t+1} = \frac{C_{j,t+1}}{C_{t+1}} &= \frac{\gamma_j a_{t+1} C_{j,t}}{a_{t+1} C_{1,t} + \gamma_2 a_{t+1} C_{2,t} + \dots + \gamma_m a_{t+1} C_{m,t}} \\ &= \frac{\gamma_j C_{j,t}/C_t}{C_{1,t}/C_t + \gamma_2 C_{2,t}/C_t + \dots + \gamma_m C_{m,t}/C_t} \\ &= \frac{\gamma_j \lambda_{j,t}}{\lambda_{1,t} + \gamma_2 \lambda_{2,t} + \dots + \gamma_m \lambda_{m,t}}, \quad j = 1, \dots, m. \end{aligned} \tag{A.1}$$

¹²According to GISAID data reported on <https://covariants.org/>

A.1 Estimation and Inference

Let $X_{j,t}$ be the number of cases that are identified as the j -th variant at times t , and assume that $(X_{1,t}, \dots, X_{m,t})$ is a representative sample of $(C_{1,t}, \dots, C_{m,t})$. The log-likelihood is now given by,

$$\ell(\gamma, \lambda_0) \propto \sum_{t=1}^T \sum_{j=1}^m X_{j,t} \log \lambda_{j,t}, \quad (\text{A.2})$$

where λ_t evolves according to (A.1) and the two vectors of unknown parameters are $\gamma = (\gamma_2, \dots, \gamma_m)'$ and the initial value $\lambda_0 \equiv (\lambda_{2,0}, \dots, \lambda_{m,0})'$. These can be estimated by maximum likelihood, $(\hat{\lambda}, \hat{\gamma}) = \arg \max_{\gamma, \lambda} \ell(\lambda, \gamma)$, and confidence intervals for λ and γ can be obtained with conventional methods. This model does not conform with the simple logistic regression model we used in the case with two variant, but could be cast as a multinomial logistic regression model.

A.2 Omitting Variants from the Analysis

For some variants, the number of observed cases may be too small to obtain reliable estimates of their relative contagiousness. An interesting question is if omitting all but two variants from the analysis will induce bias and/or inconsistencies in the estimated relative contagiousness. This is fortunately not the case. Suppose we drop variants $j = 3, \dots, m$ from the analysis and proceed to estimate γ_2 solely from data on the first two variant. Define $\tilde{\lambda}_t = C_{2,t}/(C_{1,t} + C_{2,t})$, then from (A.1) it follows that

$$\begin{aligned} \tilde{\lambda}_{t+1} &\equiv \frac{\lambda_{2,t+1}}{\lambda_{1,t+1} + \lambda_{2,t+1}} = \frac{\frac{\gamma_2 \lambda_{2,t}}{\lambda_{1,t} + \gamma_2 \lambda_{2,t} + \dots + \gamma_m \lambda_{m,t}}}{\frac{\lambda_{1,t}}{\lambda_{1,t} + \gamma_2 \lambda_{2,t} + \dots + \gamma_m \lambda_{m,t}} + \frac{\gamma_2 \lambda_{2,t}}{\lambda_{1,t} + \gamma_2 \lambda_{2,t} + \dots + \gamma_m \lambda_{m,t}}} \\ &= \frac{\gamma_2 \lambda_{2,t}}{\lambda_{1,t} + \gamma_2 \lambda_{2,t}} = \frac{\gamma_2 \frac{\lambda_{2,t}}{\lambda_{1,t} + \lambda_{2,t}}}{\frac{\lambda_{1,t}}{\lambda_{1,t} + \lambda_{2,t}} + \gamma_2 \frac{\lambda_{2,t}}{\lambda_{1,t} + \lambda_{2,t}}} = \frac{\gamma_2 \tilde{\lambda}_t}{(1 - \tilde{\lambda}_t) + \gamma_2 \tilde{\lambda}_t}, \end{aligned}$$

which is identical to (1). This shows that estimation and inference about a single relative contagiousness parameter can be based entirely on data for the two variants whose relative contagiousness is the object of interest.

Forecasting, as well as most hypothesis tests involving multiple γ -parameters, would require knowledge about the dependence between the estimates. Such situations calls for estimation of the full model defined by the log-likelihood in (A.2).

Appendix B: Robust Standard Errors of Estimators

While the log-likelihood estimates are identical to those obtained with logistic regression packages, the standard errors provided by most packages are based on the Fisher Information matrix, $\hat{\mathcal{I}}$ (defined below), and for these to be reliable, the model must be correctly specified. We will compute standard errors using the sandwich form of variance-covariance matrix for the estimated parameters, which is detailed next.

We parameterize the log-likelihood with the standard parameterization of the logistic regression, $\theta' = (\alpha, \beta) = (\log \rho_0, \log \gamma)$. The maximum likelihood estimates are obtained by maximizing $\sum_{t=1}^T \ell_t(\theta)$, where $\ell_t(\theta) = X_t \log \lambda_t + (N_t - X_t) \log(1 - \lambda_t)$. To compute robust standard errors we derive the score, $s_t(\theta) = \frac{\partial \ell_t(\theta)}{\partial \theta}$, and hessian, $h_t(\theta) = \frac{\partial^2 \ell_t(\theta)}{\partial \theta \partial \theta'}$. To this end we observe that the derivatives of $\lambda_t(\theta) = \lambda_t(\alpha, \beta) = [1 + e^{-\alpha - \beta t}]^{-1}$ are simply

$$\frac{\partial \lambda_t(\theta)}{\partial \alpha} = -e^{-\alpha - \beta t} \frac{1}{(1 + e^{-\alpha - \beta t})^2} = -\lambda_t(1 - \lambda_t),$$

and similarly of $\partial \lambda_t / \partial \beta = -\lambda_t(\theta)[1 - \lambda_t(\theta)] \times t$, such that the score for the observations in the t -th week is given

$$s_t(\theta) = [-X_t(1 - \lambda_t) + (N_t - X_t)\lambda_t] \begin{bmatrix} 1 \\ t \end{bmatrix} = (N_t \lambda_t - X_t) \begin{bmatrix} 1 \\ t \end{bmatrix}. \quad (\text{A.3})$$

Next, by combining the expression for $\partial \lambda_t(\theta) / \partial \theta$ with (A.3) we obtain,

$$h_t(\theta) = -N_t \lambda_t(1 - \lambda_t) \begin{bmatrix} 1 & t \\ t & t^2 \end{bmatrix}.$$

It is now straightforward to compute the information matrices $\hat{\mathcal{J}} = \sum_{t=1}^T s_t(\hat{\theta}) s_t(\hat{\theta})'$ and $\hat{\mathcal{I}} = -\sum_{t=1}^T h_t(\hat{\theta})$.

The likelihood is based on the assumption that $X_t | N_t \sim \text{Bin}(N_t, \lambda_t)$ and independent across time. Misspecification can arise in two ways. One way is that the binomial assumption and/or time-independence may be incorrect (distributional misspecification) and the other is dynamic misspecification where $\mathbb{E}(X_t / N_t)$ does not agree with the specified model for λ_t . Under distributional misspecification the information matrix equality need not hold, and $\hat{\mathcal{J}}$ and $\hat{\mathcal{I}}$ may have different probability limits. If the independence across t is still valid, such that s_t is not autocorrelated, then we can compute the robust variance covariance matrix for $\hat{\theta}$, with $\hat{\Sigma} = \hat{\mathcal{I}}^{-1} \hat{\mathcal{J}} \hat{\mathcal{I}}^{-1}$.¹³ If the time-independence

¹³The numerical derivatives computed by the Julia package, `ForwardDiff`, see Revels et al. (2016), are identical to the analytical expressions for both the score, $s_t(\hat{\theta})$, $t = 1, \dots, T$, and the hessian, $\sum_{t=1}^T h_t(\hat{\theta})$.

Table A.1: Sensitivity of confidence intervals for relative contagiousness.

Variance-Estimator	Alpha Variant (CI 95%)	Delta Variant (CI 95%)
$\hat{\Sigma} = \hat{\mathcal{I}}^{-1}$	$\gamma_{4.7\text{days}} \in [1.5037, 1.5262]$	$\gamma_{4.7\text{days}} \in [2.1319, 2.2033]$
$\hat{\Sigma} = \hat{\mathcal{I}}^{-1} \hat{\mathcal{J}}_0 \hat{\mathcal{I}}^{-1}$	$\gamma_{4.7\text{days}} \in [1.4994, 1.5306]$	$\gamma_{4.7\text{days}} \in [2.0215, 2.3236]$
$\hat{\Sigma} = \hat{\mathcal{I}}^{-1} \hat{\mathcal{J}}_1 \hat{\mathcal{I}}^{-1}$	$\gamma_{4.7\text{days}} \in [1.4990, 1.5310]$	$\gamma_{4.7\text{days}} \in [2.0119, 2.3347]$
$\hat{\Sigma} = \hat{\mathcal{I}}^{-1} \hat{\mathcal{J}}_2 \hat{\mathcal{I}}^{-1}$	$\gamma_{4.7\text{days}} \in [1.4986, 1.5314]$	$\gamma_{4.7\text{days}} \in [2.0009, 2.3476]$
$\hat{\Sigma} = \hat{\mathcal{I}}^{-1} \hat{\mathcal{J}}_3 \hat{\mathcal{I}}^{-1}$	$\gamma_{4.7\text{days}} \in [1.4980, 1.5320]$	$\gamma_{4.7\text{days}} \in [1.9949, 2.3546]$
$\hat{\Sigma} = \hat{\mathcal{I}}^{-1} \hat{\mathcal{J}}_4 \hat{\mathcal{I}}^{-1}$	$\gamma_{4.7\text{days}} \in [1.4971, 1.5329]$	$\gamma_{4.7\text{days}} \in [1.9909, 2.3593]$
$\hat{\Sigma} = \hat{\mathcal{I}}^{-1} \hat{\mathcal{J}}_5 \hat{\mathcal{I}}^{-1}$	$\gamma_{4.7\text{days}} \in [1.4962, 1.5339]$	$\gamma_{4.7\text{days}} \in [1.9888, 2.3618]$
$\hat{\Sigma} = \hat{\mathcal{I}}^{-1} \hat{\mathcal{J}}_6 \hat{\mathcal{I}}^{-1}$	$\gamma_{4.7\text{days}} \in [1.4952, 1.5349]$	$\gamma_{4.7\text{days}} \in [1.9888, 2.3618]$

Note: Sensitivity of confidence intervals for relative contagiousness, $\gamma_{4.7\text{days}}$, to the choice of variance-covariance estimator (computed with non-robust and various robust standard errors).

is also in question, such that the score may be autocorrelated, we can instead compute:

$$\hat{\mathcal{J}}_K = \hat{\mathcal{J}} + \sum_{j=1}^{K+1} k\left(\frac{j}{K}\right) \sum_{t=1}^{T-j} \left(s_t(\hat{\theta}) s_{t+j}(\hat{\theta})' + s_{t+j}(\hat{\theta}) s_t(\hat{\theta})' \right),$$

where $k(x)$ is a kernel function with $k(0) = 1$, $k(1) = 0$. Dynamic misspecification is more problematic, as it can result in inconsistent parameter estimates.

Our empirical results are based on the autocorrelation robust estimator, $\hat{\Sigma} = \hat{\mathcal{I}}^{-1} \hat{\mathcal{J}}_K \hat{\mathcal{I}}^{-1}$, with $K = 4$ and the Parzen kernel function for $k(\cdot)$. Standard errors and confidence intervals for α and β are given from the diagonal elements of $\hat{\Sigma}$, which we denote by $\hat{\sigma}_\alpha^2$ and $\hat{\sigma}_\beta^2$, respectively. The reported 95% confidence intervals for α and β are based on the point estimates ± 1.96 times the corresponding standard error. Those for $\gamma_{4.7\text{days}} = \exp\left(\frac{4.7}{7}\beta\right)$ are given by $\exp\left\{\frac{4.7}{7}(\hat{\beta} \pm 1.96\hat{\sigma}_\beta)\right\}$.